A consistent model for surface complexation on birnessite (d -MnO2) and its application to a column experiment.

Appelo, C.A.J.; Postma, D.

published in
Geochimica et Cosmochimica Acta
1999

DOI (link to publisher)
10.1016/S0016-7037(99)00231-8

document version
Publisher's PDF, also known as Version of record

Pergamon

Geochimica et Cosmochimica Acta, Vol. 63, No. 19/20, pp. 3039–3048, 1999

0016-7037/99 $20.00 + .00

PII S0016-7037(99)00231-8

A consistent model for surface complexation on birnessite ($-MnO_2$) and its application to a column experiment

C.A.J. Appelo[1,*,2] and D. Postma[1]

[1] Department of Geology and Geotechnical Engineering and Groundwater Research Centre, Building 204, Technical University of Denmark, DK 2800 Lyngby, Denmark
[2] Hydrochemical Consultant, Valeriusstraat 11, 1071 MB Amsterdam, Netherlands

(*Received October* 15, 1998; *accepted in revised form April* 29, 1999)

Abstract—Available surface complexation models for birnessite required the inclusion of bidentate bonds or the adsorption of cation-hydroxy complexes to account for experimentally observed H^+/M^{m+} exchange. These models contain inconsistencies and therefore the surface complexation on birnessite was re-examined. Structural data on birnessite indicate that sorption sites are located on three oxygens around a vacancy in the octahedral layer. The three oxygens together carry a charge of -2, i.e., constitute a doubly charged sorption site. Therefore a new surface complexation model was formulated using a doubly charged, diprotic, sorption site where divalent cations adsorbing via inner-sphere complexes bind to the three oxygens. Using the diprotic site concept we have remodeled the experimental data for sorption on birnessite by Murray (1975) using the surface complexation model of Dzombak and Morel (1990). Intrinsic constants for the surface complexation model were obtained with the non-linear optimization program PEST in combination with a modified version of PHREEQC (Parkhurst, 1995). The optimized model was subsequently tested against independent data sets for synthetic birnessite by Balistrieri and Murray (1982) and Wang et al. (1996). It was found to describe the experimental data well. Finally the model was tested against the results of column experiments where cations adsorbed on natural MnO_2 coated sand. In this case as well, the diprotic surface complexation model gave an excellent description of the experimental results. *Copyright © 1999 Elsevier Science Ltd*

1. INTRODUCTION

The manganese oxide birnessite (δ-MnO_2) has been extensively studied for its ion exchange properties (Buser and Graf, 1955; Murray, 1975; Loganathan et al., 1977; McKenzie, 1980; Golden et al., 1986; Tsuji et al., 1992; Le Goff et al., 1996; Wang et al., 1996; Silvester et al., 1997). Its cation exchange capacity increases almost linearly with pH over a range from pH 3 to 7.5 (Murray, 1975; Balistrieri and Murray, 1982), and the exchange coefficient for proton/alkali cation exchange increases over orders of magnitude as pH increases (Tsuji et al., 1992). This behavior is not easily captured with the classical ion exchange formulas which assume constant exchange capacity and exchange coefficients, and requires adapted formulas (Tsuji et al., 1992; Tanaka and Tsuji, 1997). The surface complexation model, which includes pH-dependent charge of the exchanger, is a more appropriate model to describe ion exchange on birnessite, and it has been applied in various forms by Balistrieri and Murray (1982), Catts and Langmuir (1986) and Smith and Jenne (1991).

However, the surface complexation models presented in these various studies are not compatible. In addition, the models contain several inconsistencies. To account for the experimentally observed H^+/M^{m+} exchange and to maintain negative charge on the oxide, Catts and Langmuir (1986) and Smith and Jenne (1991) included sorption of cation-hydroxy complexes in their surface complexation models for birnessite. As already pointed out by Balistrieri and Murray (1982), the formation of cation-hydroxy surface complexes is questionable because the adsorption of alkaline earth metals occurs well below the pH range of hydrolysis of the ions. Therefore Balistrieri and Murray (1982) included adsorption to bidentate surface sites in their model. However, the bidentate model used, and originally proposed by Davis et al. (1978), contains the peculiarity that the stoichiometric coefficient for the sorption site is different in the mass balance than in the mass action equation (Davis and Leckie, 1980; Balistrieri and Murray, 1982; Waite et al., 1994).

The coordination of the structural oxygens in the crystal structure is important for the bond strength of surface complexation of metal ions (Sposito, 1983; 1984; Davis and Kent, 1990; Hiemstra and Van Riemsdijk, 1996; Venema et al., 1996). But so far the crystal structure of birnessite has not been considered in published models of surface complexation (Balistrieri and Murray, 1982; Catts and Langmuir, 1986; Smith and Jenne, 1991). Recently more detailed information has become available concerning the structure and the properties of the sorption sites on the birnessite surface (Post and Veblen, 1990; Manceau et al., 1992; Silvester et al., 1997). Drits et al. (1997) report that in more oxidized birnessite, a sorption site consists of three oxygens around a vacancy in the octahedral layer, carrying a charge of -2 (i.e., a doubly charged sorption site).

On the background of this new structural information and because of the dissatisfactory aspects of earlier surface complexation models, we have re-examined surface complexation on birnessite. A new surface complexation model was formulated using doubly charged sorption sites, and the model was tested against available experimental data. The aim of the present work is to obtain a consistent and more generally applicable model for sorption of cations on birnessite.

*Address reprint requests to C.A.J. Appelo, Valeriusstraat 11, 1071 MB Amsterdam, Netherlands (appt@xs4all.nl).

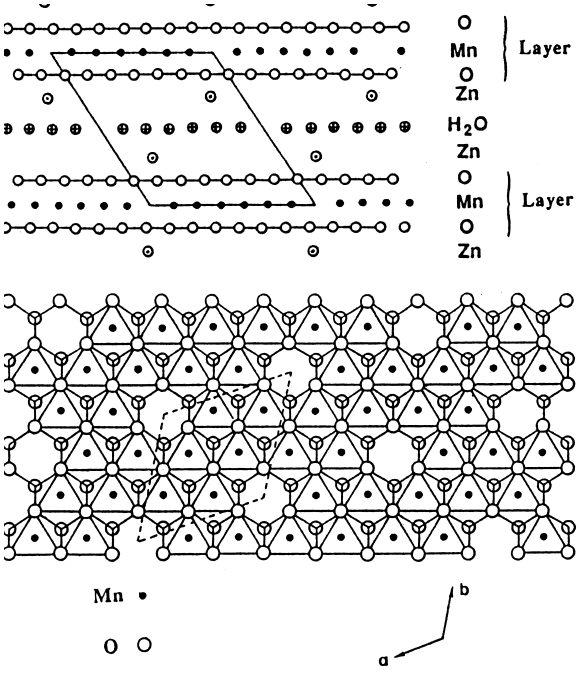

Fig. 1. The structure of chalcophanite (after Wadsley, 1955): projection along **b** (top) and along **c** (bottom) axis. Reproduced from Strobel et al. (1987).

2. CATION ADSORPTION AND THE STRUCTURE OF BIRNESSITE

Various evidence suggests that the basic structure of birnessite is similar to that of the mineral chalcophanite (Giovanoli et al., 1970a; Burns and Burns, 1979; Post and Veblen, 1990; Drits et al., 1997). Chalcophanite, $Zn_2[Mn_6\square O_{14}] \cdot 6H_2O$, consists of layers of edge sharing MnO_6 octahedra which alternate with a layer of water molecules (Wadsley, 1955; Post and Appleman, 1988). One out of seven of the Mn^{4+} positions is empty (symbol $\square$ in the structural formula), which gives a layer charge that is compensated by 2 Zn atoms located above and below the vacancy (Fig. 1).

The layer charge of chalcophanite is $-2/7 = -0.286$ per O_2. Replacement of Mn^{4+} by Mn^{3+} can create additional layer charge, to give a maximum of ~ -0.33 per O_2 in birnessite (Strobel et al., 1987; Drits et al., 1997). In fact, Post and Veblen (1990) and Drits et al. (1997) found that vacancies were almost absent in their synthetic Na-birnessites, and all the layer charge thus originated from replacement of Mn^{4+} by Mn^{3+}. Both the degree of oxidation of Mn and the layer charge are influenced by the procedures used for preparing birnessite (Bricker, 1965; Giovanoli et al., 1970a; b; McKenzie, 1971; Murray, 1974). Preparations based on MnO_4^- solutions yield more oxidized birnessite with an O/Mn >1.90. Balistrieri and Murray (1982) found an O/Mn ratio of 1.96 in their birnessite and cation exchange mainly results from the presence of vacancies. Other preparations, which start with a $Mn(OH)_2$ solution or with solid Mn_3O_4 (Bricker, 1965), initially yield a mixed Mn^{3+}/Mn^{4+} compound in which Mn^{4+} can be enriched by washing with acid. Acid washing attacks Mn^{3+} that is in a relatively weak structural position due to Jahn-Teller distortion. The Mn^{3+} either goes into the interlayer, becomes oxidized, or disproportionates to Mn^{4+} and Mn^{2+} (Giovanoli et al., 1970b; Silvester et al., 1997). The disproportionation of 2 Mn^{3+} atoms to Mn^{4+} and Mn^{2+} creates a vacancy in the octahedral layer, while Mn^{2+} goes into solution or into the interlayer.

The amount of water present in the birnessite crystal lattice depends on the ambient conditions (temperature, humidity) and on the interlayer cation (Paterson et al., 1994; Kuma et al., 1994). With either 1 or 2 layers of water molecules in the interlayer region, the c-axis spacing of birnessite is 7 or 10 Å. Na-birnessite (buserite) has a 10 Å spacing in water, which decreases to 7 Å upon drying. The process of contraction and expansion is reversible, although after numerous cycles, water uptake tends to become incomplete (Giovanoli et al., 1970a). Other alkali elements likewise give a 7 Å structure upon drying while Mg^{2+}, Ca^{2+} and Ni^{2+} forms maintain the 10 Å spacing (Golden et al., 1987; Kuma et al., 1994; Le Goff et al., 1996). Transition metal cations can also stabilize the 10 Å spacing (Golden et al., 1987; Giovanoli et al., 1975). Paterson et al. (1994) observed that, when measured wet, Na- and Ca-birnessite maintain the 10 Å spacing, while K^+ and Ba^{2+} contract to 7 Å. The effect of the various cations on the c-axis spacing must be related to cation sorption in the interlayer.

The Zn atoms in chalcophanite are associated directly with structural oxygens (Wadsley, 1955; Post and Appleman, 1988). Post and Veblen (1990) also found that Mg^{2+} is close to the structural oxygens in birnessite, but did not observe electron densities at the same location for Na- or K-birnessite. Silvester and colleagues (1997) noted corner (triple) shared Mn-O bonds, indicating that Mn^{3+} or Mn^{2+} in the interlayer was associated with structural oxygens. With EXAFS, Manceau et al. (1992) also found that transition metal cations were connected with oxygens at vacancies in the MnO_2 structure.

The structural information indicates that the sorption sites on birnessite are located inside the layer structure, as is the case for a layer-silicate such as smectite. Compared to smectite, the charge on the sorption sites on birnessite is much higher because it originates from a vacancy or charge deficiency in the direct coordination sphere of the structural oxygen, while in smectite it originates from charge deficiencies further away (in the octahedral layer). The sorbing metal ions coordinate directly to structural oxygens in birnessite (inner-sphere bonds), while in smectite they are midway in the interlayer region. The sorption sites are readily accessible for solute ions because the interlayers in birnessite contain two (or for the less hydrated cations, one) layers of water molecules. A diffuse double layer may exist outside the crystals, but it is not present in the usual sense in the interlayer region which is only 3 Å thick.

The layer charge of birnessite originates from vacancies in the octahedral layer, or from Mn^{3+} that has replaced Mn^{4+}. An oxygen at a vacancy is coordinated to 2 Mn^{4+} which provide $2 \times 4/6 = 1$ 1/3 bond valence (Pauling, 1960; Hiemstra et al., 1989; Bleam, 1993). Each oxygen has therefore an excess charge (not compensated by structural metal ions in the octahedral layer) of 2/3. The three oxygens around a vacancy have together an excess charge of $3 \times 2/3 = 2$ which can be balanced by 2 protons or a doubly charged cation in the interlayer. When the layer charge arises from Mn^{3+} in the structural layer and because Mn^{3+} occupies rows in alternation with two rows of Mn^{4+} in the ideal type II birnessite (Drits et

al., 1997), oxygens around a Mn^{3+} site are coordinated to 2 Mn^{3+} and 1 Mn^{4+} atoms. The three oxygens then have an excess charge of $3 \times 1/3 = 1$, and only one proton or alkali ion suffices. It is thus important to know whether the layer charge of the birnessite has been created by vacancies or by Mn^{3+}/Mn^{4+} replacement.

3. SURFACE COMPLEXATION MODELS

Surface complexation models for binding of metal ions on oxide surfaces comprise both monodentate and bidentate surface complexes (Davis and Kent, 1990; Dzombak and Morel, 1990; Stumm, 1992; Stumm and Morgan, 1996). For a monodentate surface complex, the reaction is:

$$\equiv SOH + M^{m+} = \equiv SOM^{(m-1)+} + H^{+}. \quad (1)$$

Here, M^{m+} is a cation that forms a monodentate complex with a surface ≡SOH. For bidentate complexation where two separate ligands (moieties) are involved, the formation of a surface complex is formally written as (Schindler et al., 1976):

$$2 \equiv SOH + N^{n+} = (\equiv SO)_2N^{(n-2)+} + 2H^{+}. \quad (2)$$

Here, N^{n+} is a cation that forms a complex with 2 ≡SOH adsorption sites. The corresponding mass action equation is

$$K_{int} = a_{(\equiv SO)_2N^{(n-2)+}}\, a^2_{H^+} / a^2_{(\equiv SOH)}\, a_{N^{n+}}, \quad (3)$$

where K_{int} represents the intrinsic constant and a_i indicates activity of species i (dimensionless). However, Balistrieri and Murray (1982) used a modification of the bidentate model which was originally advanced by Davis and Leckie (1980):

$$(\equiv SOH)_2 + N^{n+} = (\equiv SO)_2N^{(n-2)+} + 2H^{+} \quad (4)$$

with the mass action expression

$$K_{int} = a_{(\equiv SO)_2N^{(n-2)+}}\, a^2_{H^+} / a_{(\equiv SOH)_2}\, a_{N^{n+}}. \quad (5)$$

In the mass action law (Eqn. 5) the activity of the surface site has an exponent of 1 but in the mass balance for surface sites it has a stoichiometric coefficient of 2. This version of the bidentate model with a different stoichiometric coefficient in the mass balance than in the mass action equation (Davis et al., 1978; Davis and Leckie, 1978; Balistrieri and Murray, 1982; Waite et al, 1994) is somewhat awkward and thermodynamically unsatisfactory. It also requires an uncoupling of mole balances in geochemical models as is permitted in FITEQL or PHREEQC. However, in the original bidentate sorption model of Schindler et al. (1976) (Eqns. 2 and 3) the coefficients are correct and equal in the mass balance and mass action equation.

The bidentate bonds on a solid surface as described by Eqn. 4 corresponds to 2 fixed sites close together, and Eqn. 4 in reality describes sorption at a doubly charged site which may be written in a formally more correct way. As described in the previous section, the structural data on birnessite indicates that the 3 oxygens surround a vacancy with a charge of −2. Accordingly, a doubly charged multi-oxygen adsorption site can be formulated as follows:

$$\equiv SO_3H_2 + H^{+} = \equiv SO_3H_3^{+} \quad (6)$$

$$\equiv SO_3H_2 = \equiv SO_3H^{-} + H^{+} \quad (7)$$

$$\equiv SO_3H^{-} = \equiv SO_3^{2-} + H^{+} \quad (8)$$

$$\equiv SO_3^{2-} + M^{m+} = \equiv SO_3M^{(m-2)+} \quad (9)$$

$$\equiv SO_3H^{-} + M^{m+} = \equiv SO_3HM^{(m-1)+} \quad (10)$$

The notation $\equiv SO_3^{2-}$ with a total charge of −2 indicates here that the model is for the 3 oxygens around a vacancy in the octahedral layer. Adsorbing metals bind via inner-sphere complexes to the 3 oxygens. The association reactions represented by Eqns. (9) and (10) are in fact similar to complexation of metal ions to diprotic acids such as H_2CO_3 and H_2SO_4. By analogy, we may call the active sorption site in birnessite a diprotic site.

4. DERIVATION OF THE SURFACE COMPLEXATION MODEL

PHREEQC (Parkhurst, 1995) was used in conjunction with the non-linear least squares parameter estimation program PEST (Watermark Computing, http://www.pest.gil.com.au/index.html) to obtain a surface complexation model for birnessite. PEST has the advantage over FITEQL (Westall, 1982), which has been used in most other studies, that any number of parameters can be optimized (less, or equal to the number of observations). PHREEQC contains the surface complexation model of Dzombak and Morel (1990). In this model the activity of the surface species, i, is equal to the concentration, m_i in mol/kg water (Dzombak and Morel, 1990). The tacit assumption herein is that the standard state for a sorbed species is equal to the standard state for a solute ion, i.e., an ideal solution of 1 mol/kg water (Appelo and Postma, 1993). However when both monodentate and bidentate surface complexes are considered, this definition of the standard state of sorbed species gives incorrect results as illustrated below. Reactions 1 and 2 can be combined cancelling ≡SOH:

$$2 \equiv SOM^{(m-1)+} + N^{n+} = (\equiv SO)_2N^{(n-2)+} + 2\,M^{m+}, \quad (11)$$

which gives the mass action equation:

$$K_{int} = a_{(\equiv SO)_2N^{(n-2)+}}\, a_{M^{m+}} / a^2_{\equiv SOM^{(m-1)+}} a_{N^{n+}}. \quad (12)$$

Using a standard state of 1 mol/kg water for surface species and for simplicity assuming that the activity coefficients for the solute species are the same, this is numerically equivalent to:

$$K_{sw} = m_{(\equiv SO)_2N^{(n-2)+}}\, m_{M^{m+}} / m^2_{\equiv SOM^{(m-1)+}} m_{N^{n+}}. \quad (13)$$

Equation (13) has an artificial effect demonstrated by the following imaginary experiment. Consider a reaction vessel which contains a solution with solute ions M^{m+} and N^{n+} and a sorbing solid in equilibrium with that solution. Now add more solid with exactly the same surface composition. This changes the ratio $m_{(\equiv SO)_2N^{(n-2)+}} / m^2_{\equiv SOM^{(m-1)+}}$. But according to Eqn. (13), it must at the same time alter the ratio $m_{M^{m+}} / m_{N^{n+}}$ in the opposite direction. Thus the solute concentrations would change in the container when more of a solid with exactly the same equilibrium composition is added, which is obviously incorrect.

This artificial effect is absent if the standard state for sorbed species equals the total number of sites. The activity of a sorbed species is then defined as its fraction of the total number of

sites, either expressed in mol/kg solid (Schindler et al., 1976; Sposito, 1983) or as the mole fraction of sorbed species at a given type of site (Hiemstra and Van Riemsdijk, 1996). Thus the activity of a sorbed species, *i*, expressed as mole fraction is:

$$a_i = n_i/s, \tag{14}$$

where n_i represents the number of sites occupied by species *i* in mol/kg solid and *s* is the total number of sorption sites in mol/kg solid. Accordingly, the code of PHREEQC was modified to use mole fractions for sorbed species in the surface complexation model. In addition the convergence criteria for PHREEQC were improved and printing of output was adapted to provide numbers with 12 significant digits which was necessary for finding the correct numerical derivatives in the Marquardt optimization procedure used by PEST.

5. A DIPROTIC SURFACE COMPLEXATION MODEL FOR BIRNESSITE

The experiments of Murray (1975) were used to derive a set of pH dependent sorption coefficients. Murray (1975) used synthetic MnO_2 with BET surface area measured to be 260 m^2/g. He added 1 mM of $CaCl_2$, $MgSO_4$, $SrCl_2$ or $BaCl_2$ to a suspension of 0.5 g MnO_2/L^{-1} in 100 mM NaCl. The suspensions were titrated with NaOH from the point of zero charge (PZC) at pH = 2.25 to pH = 7, while taking aliquots of the solution for analysis of cations.

The basic parameters for modelling the data set are the number of sorption sites (mol/L), the surface area (m^2/mol MnO_2), and the surface complexation constants. Probable limits for the number of sorption sites and the surface area were estimated as follows. Using the formula weight of Giovanoli et al. (1970a), the 0.5 g MnO_2/L^{-1} concentration employed by Murray (1975) corresponds to 4.2 mmol MnO_2/L^{-1}. Addition of 1 mM Mn^{2+} or Cu^{2+} salt by Murray (1975) resulted in complete adsorption at pH = 7, indicating that the number of sites was larger than 1 mM. Theoretically the number of sites may vary from 0.7 mM for type I birnessite with the formula $X_{0.167}MnO_2$ to 1.4 mM for type II birnessite, with the formula $X_{0.33}MnO_2$ (Drits et al., 1997). The BET surface of 260 m^2/g corresponds to 3.1×10^4 m^2/mol. Two sides of the ideal layer structure of Mn octahedra are available for sorption, and with the unit cell surface area of $a \times b = 4.85 \times 2.8$ $Å^2$ per Mn_2O_4, the surface area is at most 8.52×10^4 m^2/mol. These estimates were set as parameter boundary values. To achieve a viable result, modelling had to be performed stepwise, with only a limited number of parameters in each step.

In the first step, the number of sites, the surface area and the deprotonation and complexation constants for Na^+ and Ca^{2+} were optimized over the pH range from 4.5 to 7.5. The number of surface sites was optimized to 1.12 mM (8.6 μmoles/m^2), well within the theoretical range. The surface area was found to be a very insensitive parameter (the jacobian is very flat), and surface area remained constant at 3.1×10^4 m^2/mol. The parameters calculated in this first step were fixed in the model.

In the second step, the constants for sorption of Mn^{2+} over the same pH range were optimized. The Mn^{2+} sorption constants were required for the subsequent optimization of protonation and Cl^- sorption parameters at the PZC of 2.25.

In the third step, the protonation and Cl^- sorption constants (which are of main importance for the PZC) were optimized to a summed charge of zero for all surface complexes at pH = 2.25, while equal amounts of Na^+ and Cl^- were sorbed to keep the PZC independent of the NaCl concentration. At this low pH, birnessite may disintegrate and release Mn^{2+} into solution and on to the sorption sites (Giovanoli et al., 1970b; Loganathan et al., 1977; Silvester et al., 1997). Therefore equilibrium with birnessite was imposed at atmospheric oxygen pressure and the Mn^{2+} sorption constants obtained in the second step were used. Actually the protonation and Cl^--complexation constants were already used in the first step. Iteration was therefore necessary after step 3. When all of the variables from steps 1–3 were included at once in the model, the optimization failed to converge. However, one iteration was sufficient and yielded only minor changes in the values of the parameters.

In the fourth step, the sorption data for the alkaline Earth metal ions were optimized as given by Murray (1975) in mol/$m^2 \times 10^6$. Only the specifically bound ions were included, without double layer contribution.

The various surface complexation models were tested against the experimental data, as previously done by Bradbury and Baeyens (1997) for smectite and Waite and colleagues (1994) and Kohler and colleagues (1996) for ferrihydrite. Monodentate surface complexation reactions did fit the experimental data of Murray (1975) poorly. The fit hardly improved when 'weak' and 'strong' sites were included. Moreover, the structure of birnessite with vacancies in the octahedral layer suggests only 1 type of sorption site. The increase of the surface charge during sorption of alkaline earth cations disfavored further sorption and the observed, almost linear increase of sorption capacity for these cations with pH could not be achieved. The inclusion of cation-hydroxy complexes (Catts and Langmuir, 1986) offers a method to reduce charging of the surface, but appears dubious for alkaline earth ions when the pH is low (Balistrieri and Murray, 1982). A bidentate surface complex [reaction (2)] was tried next. However, it did not provide a much better fit than the model with only monodentate species, apparently because the surface complex as a whole did not build up negative charge when pH increased.

Finally the use of a diprotic site model [Eqns. (6)–(10)] gave a much better fit than all the other models. This model did provide about 1 order of magnitude smaller sum of squared residuals compared to the standard monodentate complex [Eqn. (1)], and to the bidentate complex [Eqn. (2)]. The optimized constants of the diprotic surface complexation model are given in Table 1. Figure 2 compares the pH dependent adsorption of cations on birnessite predicted by the diprotic surface complexation model with the experimental data of Murray (1975) and excellent agreement is observed for Ca^{2+}, Ba^{2+}, Sr^{2+}, Mg^{2+} and Mn^{2+}. Modelled Mn^{2+} sorption levels off to 7.7×10^{-6} moles adsorbed/m^2 corresponding to adsorption of all added Mn^{2+} to the available surface area. Curiously, Murray (1975) reports the adsorption of 8.2×10^{-6} moles/m^2 at pH = 7.1 which is actually more than the theoretical upper limit. Sorption of Mn^{2+} was observed to be irreversible (desorption was incomplete) (Murray, 1975), and our calculations suggest that the solution in the Mn^{2+} sorption experiment was highly supersaturated with respect to birnessite and some precipitation of MnO_2 may have occurred. The sorption constants for Mn^{2+} are therefore tentative. Figure 3 shows pH buffering during the

Table 1. Intrinsic complexation constants for sorption of birnessite, using a diprotic site $\equiv SO_3^{2-}$, optimized for data from Murray (1975).

Reaction	log K
$\equiv SO_3H_2 + H^+ = \equiv SO_3H_3^+$	1.84
$\equiv SO_3H_2 = \equiv SO_3H^- + H^+$	−2.41
$\equiv SO_3H^- = \equiv SO_3^{2-} + H^+$	−5.54
$\equiv SO_3H_3^+ + C1^- = \equiv SO_3H_3C1$	1.44
$\equiv SO_3H^- + Na^+ = \equiv SO_3HNa$	1.00
$\equiv SO_3^{2-} + Na^+ = \equiv SO_3Na^-$	2.03
$\equiv SO_3H^- + K^+ = \equiv SO_3HK$	1.70[1]
$\equiv SO_3^{2-} + K^+ = \equiv SO_3K^-$	2.73[1]
$\equiv SO_3H^- + Mg^{2+} = \equiv SO_3HMg^+$	1.81
$\equiv SO_3^{2-} + Mg^{2+} = \equiv SO_3Mg$	2.44
$\equiv SO_3H^- + Ca^{2+} = \equiv SO_3HCa^+$	2.40
$\equiv SO_3^{2-} + Ca^{2+} = \equiv SO_3Ca$	2.86
$\equiv SO_3H^- + Sr^{2+} = \equiv SO_3HSr^+$	2.69
$\equiv SO_3^{2-} + Sr^{2+} = \equiv SO_3Sr$	3.18
$\equiv SO_3H^- + Ba^{2+} = \equiv SO_3HBa^+$	3.97
$\equiv SO_3^{2-} + Ba^{2+} = \equiv SO_3Ba$	4.18
$\equiv SO_3H^- + Mn^{2+} = \equiv SO_3HMn^+$	5.58
$\equiv SO_3^{2-} + Mn^{2+} = \equiv SO_3Mn$	5.98

[1] Estimated from Tsuji et al., 1992.

titration of birnessite in a 0.1 M NaCl solution and the effect of addition of 1 mM Mg^{2+} or Ba^{2+} (Murray, 1975). The lines are predicted by the model and are generally in good agreement with the data, although the modelled line for addition of Ba^{2+} is somewhat low.

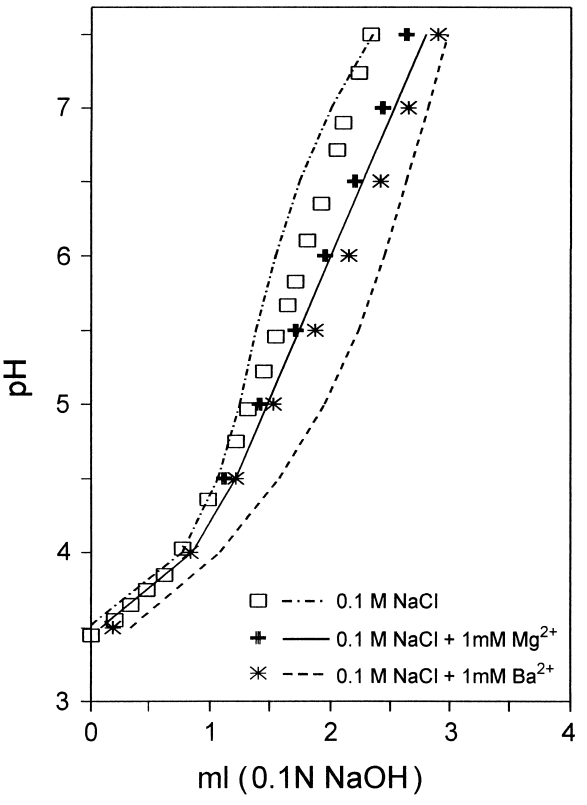

Fig. 3. pH buffering of birnessite in 0.1 M NaCl solution and with addition of 1 mM Mg^{2+} or Ba^{2+}. Experimental data are from Murray (1975); lines are predicted by the diprotic surface complexation model.

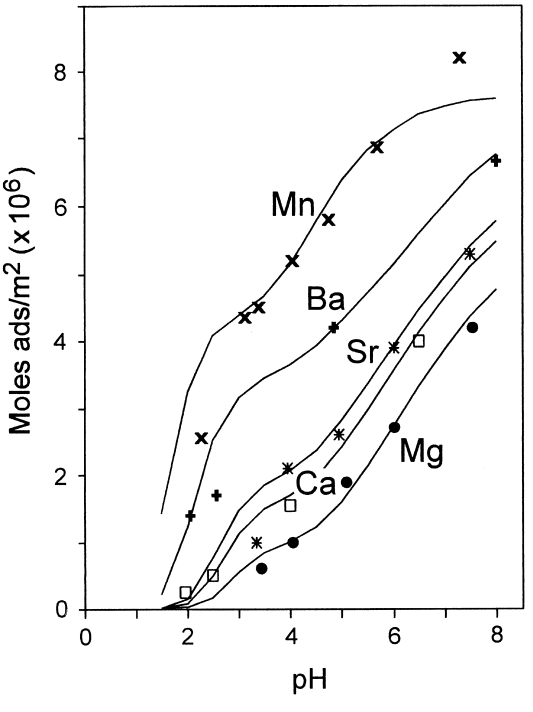

Fig. 2. pH dependent sorption of alkaline earth ions and Mn^{2+} on birnessite in a 0.1 M NaCl background solution. The concentration of alkaline earth ions is 1 mM. Experimental data are from Murray (1975) and lines are predicted by the diprotic surface complexation model.

6. MODELING OTHER SORPTION DATA ON BIRNESSITE

In order to test its general validity, the diprotic surface complexation model (Table 1) derived from the experimental results of Murray (1975) was tested against independent experimental data sets of Balistrieri and Murray (1982) and Wang and colleagues (1996). All three studies employed K- or $NaMnO_4$ solutions in the synthesis of their birnessite, which yields a highly oxidized birnessite with layer charge resulting from vacancies as discussed before and the results should therefore be comparable.

6.1. Cation Sorption by Birnessite in Seawater

Balistrieri and Murray (1982) equilibrated birnessite with seawater at various pH. Exchangeable cations were determined by dissolving the birnessite in hydroxylamine hydrochloride after equilibration. The synthetic birnessite used had a pH_{pzc} of 1.5, and pH ranged from 2 to 8.5.

The diprotic surface complexation model (Table 1) was used to calculate exchangeable Ca^{2+} and Mg^{2+} at varying pH. In the model, equilibrium with birnessite was imposed as before. The results of the calculations are shown in Fig. 4 together with the experimental data from Balistrieri and Murray (1982, their Fig.

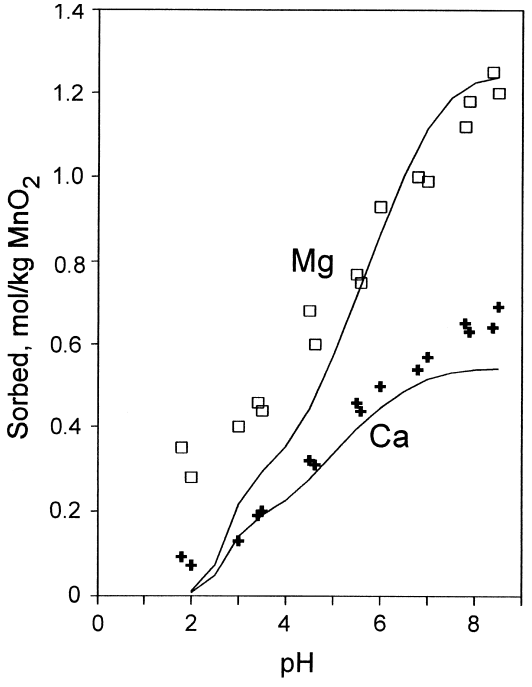

Fig. 4. Sorption of Ca^{2+} and Mg^{2+} on birnessite in seawater. Experimental data are from Balistrieri and Murray (1982) and lines are predicted by the diprotic surface complexation model.

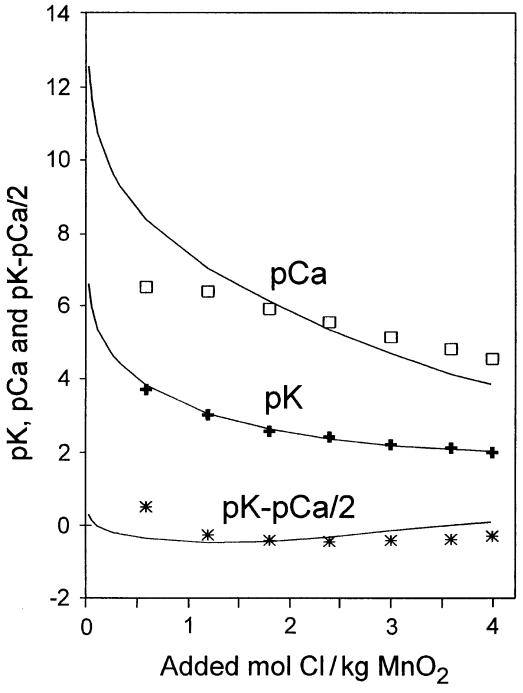

Fig. 5. The negative logarithm of K^+ and Ca^{2+} activities in solutions where K/Ca-chloride solutions are added to a suspension of synthetic Na-birnessite. Experimental data are from Wang et al. (1996) and lines are predicted by the diprotic surface complexation model.

7), and show generally good agreement. At low pH, modelled values for sorbed concentrations level off too early because the birnessite synthesized by Balistrieri and Murray (1982) had a lower PZC and therefore adsorbed more cations at low pH than the birnessite used by Murray (1975). Modeled Na^+ adsorption (not shown) is higher than measured by Balistrieri and Murray (1982). The deviation is possibly an experimental artefact. Balistrieri and Murray (1982) "slightly rinsed" their birnessite before determination of adsorbed ions. Rinsing preferentially removes monovalent ions (Appelo and Postma, 1993) and may be the cause of the deviation.

6.2. Cation Sorption by Birnessite in K/Ca-solutions

Wang and colleagues (1996) measured the E_{cell} between two ion-selective electrodes for K^+ and Ca^{2+} inserted in suspensions of synthetic Na-birnessite to which various proportions of K^+/Ca^{2+}-chloride solutions were added. Their results are displayed in Fig. 5 as the negative logarithm of ion activities as a function of the amount of $KCl/CaCl_2$ added.

The diprotic complexation model was again used to calculate pK, pCa and pK−0.5 pCa for comparison with the experimental data of Wang and colleagues (1996). The complexation constant for K^+, as listed in Table 1, was estimated to be 5 times higher than for Na^+, based on the data from Tsuji and colleagues (1992). As shown in Fig. 5 the general trends of the model prediction are in excellent agreement with the experimental data of Wang and colleagues (1996, their Fig. 4). For low additions of the K/Ca-chloride solution, the calculated pCa was higher than the measured value, apparently because Ca complexation was overestimated by the model. However, the measured pCa values are very small and may be in the range where the ion-selective electrode loses its sensitivity.

Sorption is strongly influenced by the way the birnessite is prepared. These influences are easily calculated with PHREEQC, and such calculations may be worthwhile for indicating to experimenters what the effects are of their manipulations. Wang and colleagues (1996) synthesized K-birnessite and used 0.5 M NaCl solution to convert it into the Na-form. The pH of the solution influences the fractions of $\equiv SO_3^{2-}$ and $\equiv SO_3H^-$ which are available for sorption of Na^+. Shifts up and down the vertical axis in Fig. 5 are therefore possible by adapting the pH value of the NaCl solution. In our calculations, the pH of this solution was set to 5.6 (i.e., as in equilibrium with a laboratory atmosphere with $P_{CO_2} = 10^{-3.5}$ atm).

6.3. The Applicability of the Diprotic Surface Complexation Model

The diprotic surface complexation model for birnessite was derived from the experimental data set of Murray (1975) and subsequently found to match favorably with the independent data sets of Balistrieri and Murray (1982) and Wang and colleagues (1996). Considering that three independent syntheses of birnessite are involved and also that the solution composition, and thereby the aqueous speciation, varied considerably, this is a promising result. It indicates that the proposed diprotic model for birnessite is generally applicable for cation adsorption on synthetic birnessite. In addition, the diprotic surface complexation model is consistent with the surface structure of highly oxidized birnessite. We have limited our-

Table 2. Subsequent displacements of column solutions and exchangeable concentrations in $mmol_c/L^{-1}$ *PV* (1 $mmol_c/L^{-1}$ pore volume = 0.0187 meq/100 g sediment).

Resident, mM		Injected, mM		Exchangeable, $mmol_c/L^{-1}$ *PV*	
$Ca(NO_3)_2$	10.	$MgCl_2$	11.	Ca^{2+}	47.0
$MgCl_2$	10.	$CaCl_2$	50.	Mg^{2+}	46.0
$FeCl_2$	15.	KBr	100.	Fe^{2+}	18.5

selves deliberately to sorption modelling of alkaline and alkaline earth ions only. Sorption of the transition metal ions is well known to be irreversible (Murray, 1975). Hysteresis in the sorption isotherms probably results from inclusion of the ions into the octahedral layer of the birnessite where they form a solid solution with Mn^{4+}/Mn^{3+}. The structure of birnessite (Fig. 1) allows easy uptake in the octahedral layer when the atomic radii fit. Such behavior requires a solid solution model rather than a surface complexation model. For sorption of this type, any surface complexation model will show inconsistencies when the experimental conditions are varied. Thus Catts and Langmuir (1986) observed a much greater shift of the sorption edge for Cu^{2+} and Zn^{2+}, when the solid concentration was increased, than could be explained by their model.

7. COLUMN EXPERIMENTS

In order to test the applicability of the diprotic surface complexation model on Mn-oxides present in natural sediments and in systems affected by transport, a series of column experiments was carried out. The column was packed with natural Mn-oxide coated sand and injected with a sequence of $CaCl_2$ and $MgCl_2$ solutions (Table 2) to derive the column dispersivity and the sediment exchange behavior from the breakthrough curves. In order to determine the exchange capacity associated with the Mn-oxide, the column was thereafter injected with a $FeCl_2$ solution in order to reduce all MnO_2. The remaining cation exchange capacity was determined by displacement with a KBr solution.

7.1. Materials and Methods

Mn-oxide coated sand was collected from a groundwater-fed small lake in a gravel pit near Ikast, Denmark. Black Mn-oxide coated sand forms at the water table and is apparently the result of in situ oxidation. The sand consists of grains with an average diameter of 0.24 mm covered with a uniform, but friable, blackish brown coating. X-ray diffraction of the coating material showed clear reflections at 2.44 and 1.42 Å and a broad band at 7.5 Å, corresponding to random-stacked birnessite (Giovanoli, 1980). EDAX analysis revealed the following composition: 2.36% Al_2O_3, 86.98% MnO_2, 7.00% CaO and 3.65% SiO_2. The oxidation state of manganese in the coating was determined, using the method of Murray and colleagues (1984), which yielded a O/Mn ratio of 1.77 ± 0.01.

For the column experiment, the sediment was washed with 0.1 M $Ca(NO_3)_2$ to remove fine particles, rinsed with H_2O until the electrical condictivity was 50 mS/cm, and then kept in 10 mM $Ca(NO_3)_2$. The wet sediment was packed in a perspex column of 5.22 cm inner diameter and length of 5.05 cm. The column was capped by 0.2 cm thick polyethylene plugs with radial grooves for guiding water from the inlet and to the outlet tubing. To remove gas pockets, the column was drained for water and filled with CO_2 gas. When a 10 mM $Ca(NO_3)_2$ solution was pumped into the column, the CO_2 dissolved and all the pores were effectively filled with water. The pore volume was 35.8 ml. In the ensuing experiments, solutions were pumped upward in the column with a Jasco 880-PU HPLC pump at 3 mL/hr, and the effluent was sampled with a Gilson 232 sampler. In the effluent, the concentration of Fe^{2+} was determined spectrophotometrically with Ferrozine (Stookey, 1970) and Ca, Mg, K, Mn and Fe by atomic absorption spectrophotometry on acidified samples. Cl, Br and NO_3 were determined by ion chromatography. pH was measured in a flow cell directly connected to the column outlet.

7.2. Results and Exchange Capacity

In the first experiment, a 10 mM $Ca(NO_3)_2$ solution resident in the column was displaced by a 11 mM $MgCl_2$ solution. The results are displayed in Fig. 6 and show a retardation in the Mg^{2+} breakthrough compared to Cl^-, because of the displacement of Ca^{2+} from the exchanger. In the second experiment, a resident solution of 10 mM $MgCl_2$ in the column is displaced by a 50 mM $CaCl_2$ solution. The results are presented in Fig. 7 and the increase in Cl^- concentration monitors the displacement of the resident column solution. Here retardation in Ca^{2+} is observed to follow displacement of Mg^{2+} from the exchanger.

Exchange capacities were obtained from the breakthrough curves by integrating the eluted mass according to:

$$Ex_i = \int_0^n z_i m_i \, \mathrm{d}\, PV - (z_i m_i)_{t=0} - (n-1) \times (z_i m_i)_{x=0}, \tag{15}$$

where z_i represents the charge of ion i, m_i, the concentration in the eluate ($mmol/L^{-1}$), which is integrated over eluted pore volumes *PV*, $(m_i)_{t=0}$ refers to the initial solute concentration in the column ($mmol/L^{-1}$), $(m_i)_{x=0}$, the concentration in the injected solution ($mmol/L^{-1}$), and n denotes the number of pore volumes eluted. Ex_i is obtained in $mmol_c/L^{-1}$ *PV* (per liter pore volume).

The calculated exchangeable concentrations are given in Table 2. The initial exchange capacity is 47 $mmol_c$/l *PV* when Ca^{2+} is replaced by Mg^{2+} and is in good agreement with the value of 46 $mmol_c/L^{-1}$ *PV* found when Mg^{2+} is replaced by Ca^{2+}. The final cation exchange capacity after reduction of MnO_2 amounts to 18.5 $mmol_c/L^{-1}$ *PV* and is obtained from the mass of Fe^{2+} eluted with the KBr solution. Reduction of MnO_2 by Fe^{2+} causes the precipitation of $Fe(OH)_3$ and the pH drops below 4. At this pH, $Fe(OH)_3$ has no cation exchange capacity and the residual exchange capacity can probably be ascribed to clay minerals present in the sediment. Removal of the Mn-oxide from the sediment causes a decrease in cation exchange capacity of 47 − 18.5 = 28.5 $mmol_c/L^{-1}$. This loss translates to 0.14 mol_c/mol Mn on the pristine sediment, which is similar to the exchange capacity of birnessite from the type locality (Jones and Milne, 1956).

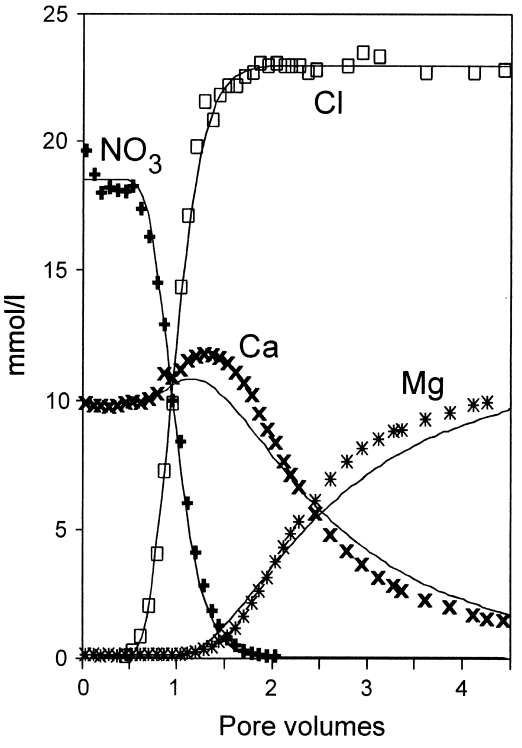

Fig. 6. Results of an experiment with a column containing sand coated with natural Mn-oxide. Breakthrough curves for displacement of a resident 10 mM $Ca(NO_3)_2$ solution in the column with a 11 mM $MgCl_2$ solution. The lines are predicted by the diprotic surface complexation model.

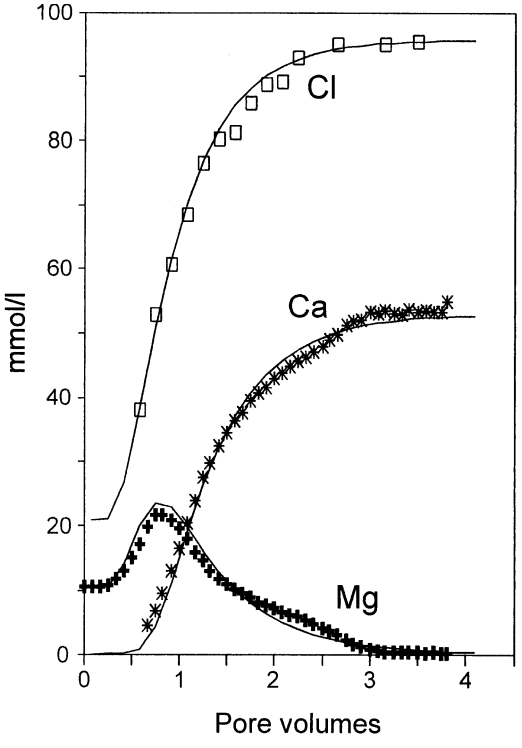

Fig. 7. Results of an experiment with a column containing sand coated with natural Mn-oxide. Breakthrough curves for displacement of a resident 10 mM $MgCl_2$ solution in the column with a 50 mM $CaCl_2$ solution. The lines are predicted by the diprotic surface complexation model.

7.3. Reactive Transport Modeling of Surface Complexation in Column Experiments

Reactive transport modelling of the column experiments was done with an adapted version of the program PHREEQC (Parkhurst, 1995) including the diprotic surface complexation model for birnessite as presented in Table 1. For the residual exchanger, the exchange coefficients for Fe^{2+}, Mn^{2+}, Ca^{2+} and Mg^{2+} were taken from Appelo and Postma (1993). The 1D transport algorithm discussed in that work was programmed in PHREEQC for solving the advection-reaction-dispersion equation (Parkhurst and Appelo, in prep.). Figures 6 and 7 compare the modelled breakthrough curves with the measured data. At the pH of the displacing solutions, Cl^- behaves as a conservative ion and front spreading for Cl^- therefore results from dispersion. Appelo and Postma (1999) evaluated dispersion behavior in these experiments and found that dispersivity depended on the cation adsorbed onto birnessite, probably related to swelling and shrinking of the mineral. When Mg^{2+} displaced Ca^{2+} from the birnessite (Fig. 6) a low dispersivity of 1.24 mm was found. However when Ca^{2+} displaced Mg^{2+}, (Fig. 7) the dispersivity increased to 8.2 mm. Accordingly, the Cl^- breakthrough curve is steep in Fig. 6 and spread over more pore volumes in Fig. 7.

The concentrations of Ca^{2+} and Mg^{2+} are well modelled which indicates that the diprotic surface complexation model, optimized on Murray's (1975) data for synthetic birnessite, is also applicable to the natural Mn-oxide present in the column sediment. Both when Mg^{2+} and Ca^{2+} are displaced from the exchanger, their concentration initially increases above the original concentration in the column and thereafter decreases to zero. This characteristic 'snow-plow' concentration profile is often found when ion exchange reactions take place in a column (Barry et al., 1983). The ions that are displaced from the exchanger initially increase in concentration to compensate for the higher anion concentration in the displacing solution and then decrease again when the exchanger becomes exhausted.

The breakthrough curve of the exchanged cations following the snow-plow is related to the shape of the exchange isotherm (Appelo, 1996). If the eluted ion is more strongly bound than the displacing ion, the slope of the sorption isotherm dq/dc is lower for higher than for lower concentrations (the isotherm is convex). Retardation increases for lower concentrations and a broadening front is the result. If the isotherm is concave for the eluted ion, the front sharpens because lower concentrations have smaller retardation than higher concentrations. The effects of sharpening and broadening can be observed in Figs. 6 and 7. Ca^{2+} is bound more strongly than Mg^{2+} by birnessite (Table 1) and the Ca/Mg isotherm is thus convex for Ca^{2+}. Low concentrations of Ca^{2+} are therefore retarded more strongly than higher concentrations. Accordingly, the displacement of Ca^{2+} by Mg^{2+} (Fig. 6) shows broader breakthrough curves for cations than for Cl^-. Conversely for displacement of Mg^{2+} by Ca^{2+} (Fig. 7), the cation breakthrough curves become slightly steeper than for Cl^-.

8. CONCLUSIONS

Structural data on birnessite surface coordination indicate that sorption sites consist of three oxygens around a vacancy in the octahedral layer, carrying a charge of −2 (i.e., a doubly charged sorption site where metals adsorbing via inner-sphere complexes bind to the three oxygens).

A new surface complexation model was formulated using a doubly charged, diprotic, sorption site and optimized using the set of experimental data for sorption on birnessite of Murray (1975).

The optimized model was subsequently tested against independent data sets for synthetic birnessite by Balistrieri and Murray (1982) and Wang and colleagues (1996) and found to describe the experimental data well. It appears to be generally applicable for highly oxidized synthetic birnessite.

The model was also tested by reactive transport modelling of the results of column experiments where cations adsorbed on natural MnO_2 coated sand. In this case as well, the diprotic surface complexation model gave an excellent description of the experimental results.

Acknowledgments—We thank Henrik Skov for expertly doing the chemical analysis of the column experiments solutions.

REFERENCES

Appelo C. A. J. (1996) Multicomponent ion exchange and chromatography in natural systems. In *Reactive Transport in Porous Media* (eds. P. C. Lichtner, C. I. Steefel and E. H. Oelkers) *Reviews in Mineralogy* **Vol. 34,** 193–227. Miner. Soc. Amer.

Appelo C. A. J. and Postma D. (1993) *Geochemistry, Groundwater and Pollution.* Balkema

Appelo C. A. J. and Postma D. (1999) Variable dispersivity in a column experiment containing MnO_2 and FeOOH coated sand. *J.Contam. Hydrol.* (in press).

Balistrieri L. S. and Murray J. W. (1982) The surface chemistry of (MnO_2 in major ion seawater. *Geochim. Cosmochim. Acta*. **46,** 1041–1052.

Barry D. A., Starr J. L., Parlange J.-Y., and Braddock R. D. (1983) Numerical analysis of the snow-plow effect. *Soil Sci. Soc. Am. J.* **47,** 862–868.

Bleam W. F. (1993) On modelling proton affinity at the oxide/water interface. *J. Coll. Interf. Sci.* **159,** 312–318.

Bradbury M. H. and Baeyens B. (1997) A mechanistic description of Ni- and Zn-sorption on Na-montmorillonite. II. Modelling. *J. Contam. Hydrol.* **27,** 223–248.

Bricker O. (1965) Some stability relations in the system Mn-O_2-H_2O at 25°C and one atmosphere total pressure. *Amer. Mineral.* **50,** 1296–1354.

Burns R. G. and Burns V. M. (1979) Manganese oxides. In *Marine Minerals* (ed. R. G. Burns) *Rev. Mineral.* **Vol. 6,** pp. 1–46. Miner. Soc. Amer.

Buser W. and Graf P. (1955) Radiochemische Untersuchungen an Festkörpern III. Ionen- und Isotopenaustauschreaktionen an Mangandioxyden und Manganiten. *Helv. Chim. Acta* **92,** 810–829.

Catts J. G. and Langmuir D. (1986) Adsorption of Cu, Pb and Zn by δMnO_2: Applicability of the site binding-surface complexation model. *Applied Geochem.* **1,** 255–264.

Davis J. A. and Kent D. B. (1990) Surface complexation modeling in aqueous geochemistry. In *Mineral-Water Interface Geochemistry* (eds. M. F. Hochella, Jr. and A. F. White) *Rev. Mineral.* **Vol. 23,** pp. 177–260. Miner. Soc. Amer.

Davis J. A. and Leckie J. O. (1978) Surface ionization and complexation at the oxide/water interface. II. Surface properties of amorphous iron oxyhydroxide and adsorption of metal ions. *J. Coll. Interf. Sci.* **67,** 90–107.

Davis J. A. and Leckie J. O. (1980) Surface ionization and complexation at the oxide/water interface. III. Adsorption of anions. *J. Coll. Interf. Sci.* **74,** 32–43.

Davis J. A., James R. O., and Leckie J. O. (1978) Surface ionization and complexation at the oxide/water interface. I. Computation of electrical double layer properties in simple electrolytes. *J. Coll. Interf. Sci.* **63,** 480–499.

Drits V. A., Silvester E., Gorshkov A. I., and Manceau, A. (1997) Structure of synthetic monoclinic Na-rich birnessite and hexagonal birnessite: I. Results from X-ray diffraction and selected-area electron diffraction. *Amer. Mineral.* **82,** 946–961.

Dzombak D. A. and Morel F. M. M. (1990) *Surface Complexation Modeling-Hydrous Ferric Oxide.* Wiley.

Giovanoli R. (1980) Vernadite is random stacked birnessite. *Mineral. Deposita* **15,** 251–253.

Giovanoli R., Stähli E., and Feitknecht W. (1970a) Über Oxidhydroxide des vierwertigen Mangans mit Schichtengitter. 1. Natriummangan(II,III)manganat(IV). *Helv. Chim. Acta* **53,** 209–220.

Giovanoli R., Stähli E., and Feitknecht W. (1970b) Über Oxidhydroxide des vierwertigen Mangans mit Schichtengitter. 2. Mangan(III)-manganat(IV). *Helv. Chim. Acta* **53,** 453–464.

Giovanoli R., Bürki P., Giuffredi M., and Stumm W. (1975) Layer structured manganese oxide hydroxides. IV: The buserite group; structure stabilization by transition elements. *Chimia* **29,** 517–520.

Golden D. C., Dixon J. B., and Chen C. C. (1986) Ion exchange, thermal transformations, and oxidizing properties of birnessite. *Clays Clay Minerals* **34,** 511–520.

Golden D. C., Chen C. C., and Dixon J. B. (1987) Transformation of birnessite to buserite, todorokite, and manganite under mild hydrothermal treatment. *Clays Clay Minerals* **35,** 271–280.

Hiemstra T. and Van Riemsdijk W. H. (1996) A surface structural approach to ion adsorption: The charge distribution (CD) model. *J. Coll. Interf. Sci.* **179,** 488–508.

Hiemstra T., Van Riemsdijk W. H., and Bolt G. H. (1989) Multisite proton adsorption modeling at the solid/solution interface of (Hydr)oxides: A new approach, 1. Model description and evaluation. *J. Coll. Interf. Sci.* **133,** 91–104.

Jones L. H. P. and Milne A. A. (1956) Birnessite, a new manganese oxide mineral from Aberdeenshire, Scotland. *Mineral. Mag.* **31,** 283–288.

Kohler M., Curtis G. P., Kent D. B., and Davis J. A. (1996) Experimental investigation and modeling of uranium(VI) transport under variable chemical conditions. *Water Resour. Res.* **32,** 3539–3551.

Kuma K., Usui A., Paplawsky W., Gedulin B., and Arrhenius G. (1994) Crystal structures of synthetic 7 Å and 10 Å manganites substituted by mono- and divalent cations. *Mineral. Mag.* **58,** 425–447.

Le Goff P., Baffier N., Bach S., and Pereira-Ramos J. P. (1996) Synthesis, ion exchange and electrochemical properties of lamellar phyllomanganites of the birnessite group. *Mater. Res. Bull.* **31,** 63–75.

Loganathan P., Burau R. G., and Fuerstenau D. W. (1977) Influence of pH on the sorption of Co^{2+}, Zn^{2+} and Ca^{2+} by a hydrous manganese oxide. *Soil Sci. Soc. Am. J.* **41,** 57–62.

Manceau A., Gorshov A. I., and Drits V. A. (1992) Structural chemistry of Mn, Fe, Co and Ni in manganese hydrous oxides. Part II. Information from EXAFS spectroscopy and electron and X-ray diffraction. *Amer. Mineral.* **77,** 1144–1157.

McKenzie R. M. (1971) The synthesis of birnessite, cryptomelane, and some other oxides and hydroxides of manganese. *Mineral. Mag.* **38,** 493–502.

McKenzie R. M. (1980) The adsorption of lead and other heavy metals on oxides of manganese and iron. *Aust. J. Soil Res.* **18,** 61–73.

Murray J. W. (1974) The surface chemistry of hydrous manganese dioxide. *J. Coll. Interf. Sci.* **46,** 357–371.

Murray J. W. (1975) The interaction of metal ions at the manganese dioxide-solution interface. *Geochim. Cosmochim. Acta* **39,** 505–519.

Murray J. W., Balistrieri L. S., and Paul B. (1984) The oxidation state of manganese in marine sediments and ferromanganese nodules. *Geochim. Cosmochim. Acta* **48,** 1237–1247.

Parkhurst D. L. (1995) User's guide to PHREEQC-a computer program for speciation, reaction-path, advective-transport, and inverse geochemical calculations. *US Geol. Surv. Water Resour. Inv. Rep. 95-4227*, 143 pp.

Parkhurst D. L. and Appelo C. A. J. (1999) User's guide to PHREEQC (version 2). *US Geol. Surv. Water Resour. Inv. Rep.* in prep.

Paterson E., Swaffield R., and Clark L. (1994) The influence of structure on Ba and K uptake by a synthetic phyllomanganate. *Clay Min.* **29,** 215–222.

Pauling L. (1960) *The nature of the chemical bond.* 3rd. ed. Cornell Univ. Press.

Post J. E. and Appleman D. E. (1988) Chalcophanite, $ZnMn_3O_7 \cdot 3H_2O$: New crystal-structure determinations. *Amer. Mineral.* **73,** 1401–1404.

Post J. E. and Veblen D. R. (1990) Crystal structure determinations of synthetic sodium, magnesium, and potassium birnessite using TEM and the Rietveld method. *Amer. Mineral.* **75,** 477–489.

Schindler P. W., Fürst B., Dick R., and Wolf P. U. (1976) Ligand properties of surface silanol groups. 1. Surface complex formation with Fe^{3+}, Cu^{2+}, Cd^{2+} and Pb^{2+}. *J. Coll. Interf. Sci.* **55,** 469–475.

Silvester E., Manceau A., and Drits V. A. (1997) Structure of synthetic monoclinic Na-rich birnessite and hexagonal birnessite: II. Results from chemical studies and EXAFS spectroscopy. *Amer. Mineral.* **82,** 962–978.

Smith R. W. and Jenne E. A. (1991) Recalculation, evaluation, and prediction of surface complexation constants for metal adsorption on iron and manganese oxides. *Environ. Sci. Technol.* **25,** 525–531.

Sposito G. (1983) On the surface complexation model of the oxide-aqueous solution interface. *J. Coll. Interf. Sci.* **91,** 329–340.

Sposito G. (1984) *The surface chemistry of soils.* Oxford Univ. Press

Stookey L. L. (1970) Ferrozine-A new spectrophotometric reagent for iron. *Anal. Chem.* **42,** 779–781.

Strobel P., Charenton J.-C., and Lenglet M. (1987) Structural chemistry of phyllomanganates: Experimental evidence and structural models. *Rev. Chim. Min.* **24,** 199–220.

Stumm W. (1992) *Chemistry of the solid-water interface.* Wiley.

Stumm W. and Morgan J. J. (1996) *Aquatic Chemistry, 3rd. ed.* Wiley.

Tanaka Y. and Tsuji M. (1997) Thermodynamic study of alkali metal ion exchange on a manganese dioxide with hexagonal structure. *Mat. Res. Bull.* **32,** 461–475.

Tsuji M., Komarneni S., Tamaura Y., and Abe M. (1992) Cation exchange properties of a layered manganic acid. *Mat. Res. Bull.* **27,** 741–751.

Venema P., Hiemstra T., and Van Riemsdijk W. H. (1996) Multi site adsorption of cadmium on goethite. *J. Coll. Interf. Sci.* **183,** 515–527.

Wadsley A. D. (1955) The crystal structure of Chalcophanite, $ZnMn_3O_7 \cdot 3H_2O$. *Acta Cryst.* **8,** 165–172.

Waite T. D., Davis J. A., Payne T. E., Waychunas G. A. and Xu N. (1994) Uranium(VI) adsorption to ferrihydrite: Application of a surface complexation model. *Geochim. Cosmochim. Acta* **58,** 5465–5478.

Wang F. L., Yu T. R., Huang P. M., Krishnamurti G. S. R., Li S. X., and Fairhurst D. (1996) Competitive adsorption of potassium and calcium on manganese oxide as studied with two ion-selective electrodes. *Z. Pflanzenern. Bodenk.* **159,** 93–99.

Westall J. C. (1982) FITEQL. A program for the determination of chemical equilibrium constants from experimental data, user's guide, version 2.0. Chem. Dept., Oregon State Univ.